# Structure of Physical Gels Formed in Syndiotactic Polystyrene/Solvent Systems Studied by Small-Angle Neutron Scattering

**Masamichi Kobayashi,* Toshinori Yoshioka, Takehito Kozasa, and Kohji Tashiro**

*Department of Macromolecular Science, Faculty of Science, Osaka University, Toyonaka, Osaka 560, Japan*

**Jun-ichi Suzuki and Satoru Funahashi**

*Department of Materials Science and Engineering, Japan Atomic Energy Research Institute, Tokai, Ibaraki 319-11, Japan*

**Yoshinobu Izumi**

*Macromolecular Research Laboratory, Faculty of Engineering, Yamagata University, Yonezawa, Yamagata 992, Japan*

*Received October 19, 1993*•

ABSTRACT: The molecular aggregation state in physical gels of syndiotactic polystyrene (SPS) dispersed in various organic solvents was investigated by means of small-angle neutron scattering (SANS). The SANS intensity profiles measured for the momentum transfer $q$ range of 0.02–2.0 $nm^{-1}$ were reproduced well by the equation derived by Freltoft, Kjems, and Sinha for describing SANS profiles of fractal objects. The relevant structural parameters such as the correlation length (the upper cutoff length) $\xi$, the lower cutoff length $r_0$, the mass fractal dimension $D_m$, and the surface fractal dimension $D_s$ were obtained from the least-squares fittings to the data. The SANS profiles measured at 25 °C, and the structural parameters derived from them, varied depending on the solvent in which SPS molecules were dispersed. In particular, the profile of SPS/chloroform gel differed remarkably from those of SPS/*o*-dichlorobenzene and SPS/carbon tetrachloride gels. The obtained structural parameters suggested that, in SPS/chloroform gel, the coagulates of polymer segments were less-developed, forming loosely packed clusters compared with the latter two cases. The result was consistent with the fact revealed by infrared spectroscopy that the orderliness of the TTGG skeletal conformation of polymer molecules in SPS/chloroform gels at room temperature is far less than that in SPS/*o*-dichlorobenzene and SPS/$CCl_4$ gels. The SANS profiles were analyzed also by other commonly used methods such as the Guinier plot, the Kratky plot, and the Zimm plot, and their usefulness was considered.

## Introduction

Syndiotatic polystyrene (SPS) is the counterpart of isotactic polystyrene (IPS) which is well-known as the first synthetic stereoregular polymer.[1] In crystalline phases, IPS molecules assume a (3/1) helical form consisting of a regular repetition of the *trans* (T) and *gauche* (G) conformations of the skeletal C–C bonds. There are two stable conformations in crystalline SPS, the TT type ($\alpha$ form) that constructs a fully extended zigzag chain and the TTGG type ($\beta$ form) constructing a (2/1) helix, although two or more crystal modifications have been found so far for each type.[2-9] In previous papers,[10-12] we have demonstrated that stable transparent gels are formed by allowing SPS solutions prepared at elevated temperatures to stand at room temperature. Infrared spectra taken on the SPS gels indicated that highly ordered TTGG skeletal conformations were formed on gelation even at polymer concentrations as low as 0.1 g/dL. It has been shown that static and dynamic behaviors of the conformational ordering on gelation depend to a great extent on the kind of solvent in which SPS molecules are dispersed, although the resultant ordered conformation is the same TTGG type regardless of the solvent.[13,14] For example, in the case of *o*-dichlorobenzene (*o*-DCB) and carbon tetrachloride ($CCl_4$) solutions, gelation is completed within a few minutes at 25 °C and the conformational order reaches a large extent (more than 80% of monomeric units are accommodated in regular TTGG sequences containing 8 or more monomeric units) even below the macroscopic critical overlap polymer concentration $C^*$. In the case of a chloroform solution, on the contrary, the gelation proceeds very slowly (with the time scale of several tens of hours at 10 °C), the conformational ordering takes place only above $C^*$, and the orderliness is limited to a low level compared with the former two cases.

There are experimental evidences suggesting that the ordered TTGG conformation of SPS molecules in gels as well as in solids is stabilized by the presence of solvent molecules, presumably by the formation of polymer–solvent complexes.[11] Therefore, the difference in gelation behaviors mentioned above is considered to be attributed to a difference in the polymer–solvent interactions among various SPS/solvent systems. The main subject of the present work is to clarify the solvent effect on the aggregation state of SPS molecules formed in gels.

The small-angle neutron scattering (SANS) is one of the powerful methods used to investigate structures of molecular aggregates or clusters formed in gels, in particular those with several tens of nanometers length scales. In the present work, SANS experiments were performed on SPS gels dispersed in three different solvents, *o*-dichlorobenzene (*o*-DCB), carbon tetrachloride, and chloroform at 25 °C. The relevant structural parameters describing the state of aggregation were derived through quantitative analyses of the measured SANS intensity profiles.

## Experimental Section

**A. Samples.** The SPS samples were supplied from Idemitsu Kosan Co. Ltd. and used without further fractionation. The weight-average molecular weights $M_w$ (by GPC) were $15 \times 10^4$,

• Abstract published in *Advance ACS Abstracts*, February 1, 1994.

0024-9297/94/2227-1349$04.50/0 

$36 \times 10^4$, $40 \times 10^4$, and $113.5 \times 10^4$. The fully deuterated SPS sample (SPS-$d_8$) with $M_w = 24.8 \times 10^4$ was prepared by polymerization of styrene-$d_8$ according to the procedure reported by Ishihara et al.[15] The solvents used were deuterated *o*-DCB (*o*-$C_6D_4Cl_2$), deuterated chloroform ($CDCl_3$), and carbon tetrachloride ($CCl_4$). A preset amount of SPS (or SPS-$d_8$ for the case of $CCl_4$ gels) was sealed with solvent in a glass ampule. The polymer was dissolved by heating the ampule on a heating plate kept at about 100 °C (above the boiling points of $CDCl_3$ and $CCl_4$). On cooling the solution down to room temperature, a transparent gel was formed in the sealed ampule. The polymer concentration $C$ in the resultant gel was determined from the amounts of the polymer and the solvent weighed into the ampule.

As the sample cells for the SANS experiments, pairs of sealed-type quartz cells with optical path lengths of 2.0, 3.0, and 5.0 mm were used depending on the polymer concentration. The gel held in a sealed glass ampule was dissolved and transferred into a quartz cell using a syringe kept at an elevated temperature to keep the sample from gelating during the transfer. The sample transferred into the quartz cell was sealed with a Teflon stopper and heated again until being dissolved. By standing the solution at room temperature, a gelatinous material, filling uniformly the cell, was obtained. The sample thus prepared along with the pure solvent filled in another quartz cell of the same optical path length was subjected to the SANS measurements.

**B. SANS Measurements.** The SANS experiments were carried out in Tokai Research Establishment of Japan Atomic Energy Research Institute using the SANS instrument situated at the end of a cold-neutron guide tube from the JRR-3 reactor. For the present experiment, neutron wavelength $\lambda = 0.625$ nm was used. The distance ($L$) from the sample to the two-dimensional position-sensitive detector (PSD) was set at 10.0 and 1.5 m. Data taken at $L = 10.0$ m cover the momentum transfer $q$ range of 0.02–0.30 $nm^{-1}$, and data taken at $L = 1.5$ m cover $q = 0.2$–$2.0$ $nm^{-1}$. Here, the $q$ is related to the Bragg angle $\theta$ by $q = (4\pi/\lambda) \sin\theta$. For some samples the distance $L$ was set at 4.0 m, covering the $q$ range of 0.08–0.70 $nm^{-1}$. For every pair of gel and solvent, the scattering intensities as a function of $q$ and the transmissions for the neutron beam, $T_{gel}$ and $T_{solv}$, were measured. After background (noise) and normalization corrections, the intensity data recorded on the two-dimensional PSD were radially averaged, resulting in scattering functions of $I(q)_{gel}$ and $I(q)_{solv}$. The scattering function for the solvent was subtracted from that of the gel according to the equation

$$I(q) = I(q)_{gel} - I(q)_{solv}(T_{gel}/T_{solv}) \quad (1)$$

giving the corrected scattering function $I(q)$ due to the polymeric clusters embedded in a solvent matrix.

## Theoretical Background

The obtained scattering profiles were analyzed according to the theory developed by Freltoft et al.[16] Polymeric clusters formed in gels were treated as fractal objects whose geometrical arrangement was described with such structural parameters as the correlation length $\xi$ (the large cutoff length on which the clusters are nonuniform), the radius of unit particles constructing the cluster $r_0$ (the short cutoff length), the mass fractal dimension within the cluster $D_m$, and the surface fractal dimension $D_s$ of the unit particles. Their physical meanings will be described in what follows.

We consider neutron scattering from a cluster consisting of $N$ unit particles. Here, the unit particle means the smallest structural unit that can be approximated by a uniform sphere. In the present case, it corresponds to a coagulate of polymer segments that works as a cross link of the gel network. The SANS profile $I(q)$ per particle is given by

$$I(q) = v_0^2(\rho_S - \rho_0)^2 f^2(q) S(q) \quad (2)$$

$$= B f^2(q) S(q) \quad (2')$$

where $\rho_s$ is the scattering length averaged over one unit particle of volume $v_0$, $\rho_0$ that of the embedding medium, $B$ a proportionality constant, and $f(q)$ the single-particle form factor which is approximated by the equation

$$f^2(q) = \exp(-q^2 r_0^2/5) \quad (3)$$

$S(q)$ is the structure factor of the particle centers located in the cluster and written in terms of the particle pair-correlation function $G(r)$ as

$$S(q) = N \int G(r) \exp(-iqr)\, dr \quad (4)$$

$$G(r) = \delta(r) + G_{diff}(r) \quad (5)$$

Here, $\delta(r)$ is the $\delta$ function and $G_{diff}(r)$ is expressed by

$$G_{diff}(r) = (A/r^{3-D_m}) \exp(-r/\xi) \quad (6)$$

Through the Fourier transformation of $G(r)$, we get the equation

$$S(q) = 1 + K\Gamma(D_m - 1)\xi^{D_m} \sin[(D_m - 1)\tan^{-1}(q\xi)]/(1 + q^2\xi^2)^{(D_m-1)/2} \quad (7)$$

where $K$ is a constant and $\Gamma(x)$ is the $\Gamma$ function of the variable $x$.

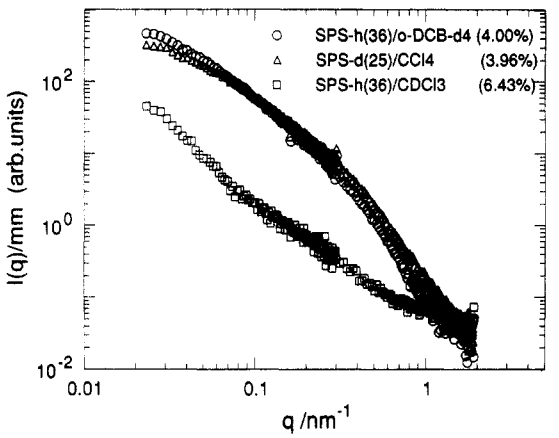


**Figure 1.** SANS intensity functions of SPS ($M_w = 36 \times 10^4$) or SPS-$d_8$ ($M_w = 25 \times 10^4$) gels dispersed in three different solvents, measured at 25 °C with a cold neutron beam of $\lambda = 0.625$ nm and the PSD positioned at 10.0 and 1.5 m apart from the sample.

## Analyses of Experimental Data

Equation 2′ together with eqs 3 and 7 was used to make nonlinear least-squares fits to the corrected SANS profiles $I(q)$. For each SPS gel, the $I(q)$ data obtained with the PSD located at $L = 10.0$ m and $L = 1.5$ m were combined as shown in Figures 1 and 2. Here, the ordinates represent the $I(q)$ value per unit path length (1 mm) of the sample cell. Two sets of data superpose each other in the common $q$ range. The data points, which are situated in the vicinity of the boundaries of the respective available $q$ ranges and largely scattered from the common intensity curve, were omitted from the least-squares fitting. Figure 3 shows an example of the least-squares fitting to the data of an SPS-$d_8$/$CCl_4$ gel. In the whole $q$ range except for the very large $q$ region, the theoretical curve reproduces well the experimental data. The obtained structural parameters are listed in Table 1 together with those of other samples. The $q$ positions corresponding to the large and short cutoff lengths are indicated in the figure. For very large $q$, the SANS profile gives rise to Porod-type characteristics; i.e., $I(q)$ is proportional to $q^{-(6-D_s)}$, and the surface fractal

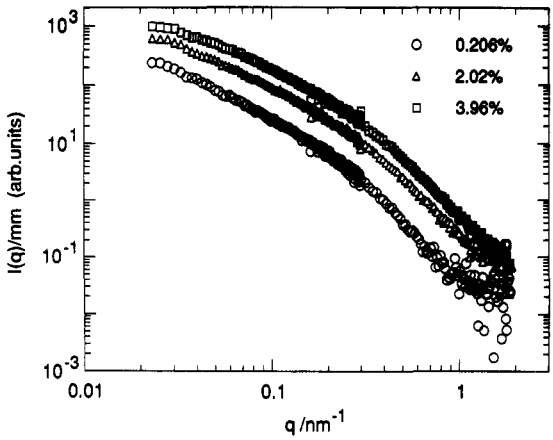


**Figure 2.** SANS intensity functions of SPS-$d_8$ ($M_w = 25 \times 10^4$)/$CCl_4$ gels at polymer concentrations of (a) $C = 3.96$, (b) 2.02, and (c) 0.206 g/dL, measured at 25 °C with a cold neutron beam of $\lambda = 0.625$ nm and the PSD positioned at 10.0 and 1.5 m apart from the sample.

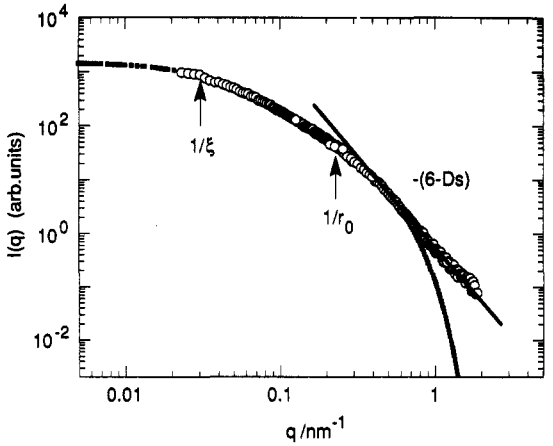


**Figure 3.** Least-squares fitting of eq 2′ (with eqs 3 and 7) to the measured $I(q)$ vs $q$ curves for an SPS-$d_8$ ($M_w = 25 \times 10^4$)/$CCl_4$ gel ($C = 4.00$ g/dL at 25 °C). The positions of $\xi$ and $r_0$ values obtained are indicated by the arrows.

**Table 1. Structural Parameters for SPS Gels Dispersed in Various Solvents Evaluated by Least-Squares Fits of Eq 2′ to SANS Data Measured with PSD Located at 10.0 and 1.5 m**

| $M_w$ | solvent | $C$ (g/dL) | $r_0$ (nm) | $D_m$ | $\xi$ (nm) | $D_s$ |
|---|---|---|---|---|---|---|
| 360 K | o-DCB | 4.00 | 2.938 | 2.066 | 33.32 | 2.124 |
| 360 K | $CDCl_3$ | 6.43 | 0.0089 | 2.409 | 56.97 | |
| 248 K | $CCl_4$ | 3.96 | 4.382 | 1.745 | 33.37 | 2.811 |

dimension $D_s$ of the unit particles can be obtained from the slope of log $I(q)$ versus log $q$.

Figure 4 shows the theoretical curves fitted to the $I(q)$ data of SPS gels dispersed in three different solvents. In the double-logarithmic plot, the fits between the theoretical and experimental results for $q$ greater than 1.0 nm$^{-1}$ seem not satisfactory, although the discrepancy is very small in the linear scale. The discrepancy comes partly from neglect of the impingement effect among unit particles [$G_{diff}(r)$ should vanish for $r \leq 2r_0$].[16] The shapes of the $I(q)$ function as well as the values of the structural parameters (Table 1) are similar to each other between SPS/o-DCB-$d_4$ and SPS-$d_8$/$CCl_4$ gels, although small differences are seen for $r_0$, $D_m$, and $D_s$.

On the contrary, SPS/$CDCl_3$ gel gives rise to an $I(q)$ profile different from those of the former two cases. Equation 7 seems unsuitable to interpret the $I(q)$ data, because the least-squares fitting gives a physically unacceptable small $r_0$ value ($r_0 < 0.1$ nm) and an anomalously

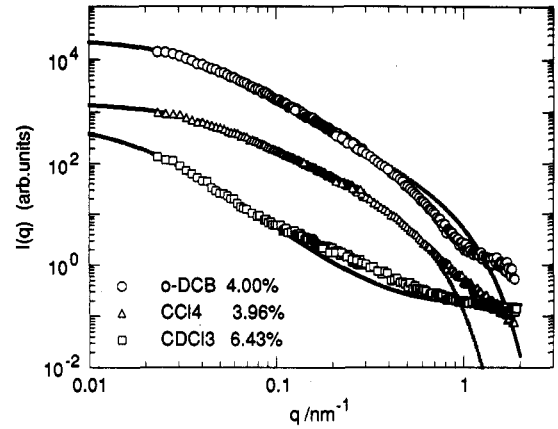


**Figure 4.** Least-squares fitting of eq 2′ (with eqs 3 and 7) to the measured $I(q)$ vs $q$ curves shown in Figure 1.

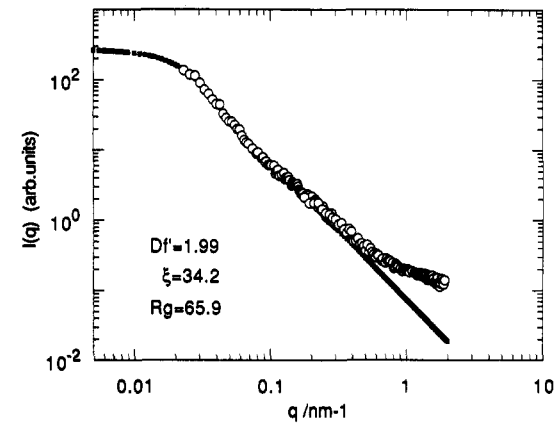


**Figure 5.** Least-squares fitting of eq 8 to the measured $I(q)$ vs $q$ curves for an SPS ($M_w = 36 \times 10^4$)/$CDCl_3$ gel ($C = 6.43$ g/dL at 25 °C). The values of structural parameters obtained are indicated.

large $\xi$ value. Therefore, the value of $D_m$ (=2.409) obtained is also questionable. As will be mentioned in the next section, the intensity data of this sample give a sol-like Kratky plot, in contrast to the cases of SPS/o-DCB-$d_4$ and SPS-$d_8$/$CCl_4$ gels which cause Kratky plots typical of the gel state. As has been described in the Introduction, gelation of the SPS/$CDCl_3$ system proceeds very slowly at room temperature. Through a recent time-resolved SANS study,[17] we have demonstrated that the same sample at an early stage of gelation gives rise to a characteristic $I(q)$ profile which can be fitted to the theoretical equation for semidilute solutions of star polymers derived by Dozier et al.[18] This is expressed as

$$I(q) = I(0)\exp(-q^2R_g^2/3) + K\Gamma(D'_m - 1) \times \sin[(D'_m - 1)\tan^{-1}(q\xi')]/q\xi'[1 + q^2\xi'^2]^{(D'_m-1)/2} \quad (8)$$

where $R_g$ represents the radius of gyration of stars and $\xi'$ and $D'_m$ are the correlation length and the mass fractal dimension, respectively, inside the star. The reciprocal of $D'_m$ is the Flory exponent $\nu(1/\nu = D'_m)$. From the definition it is noted that $R_g$ should be greater than $\xi'$.

The present SANS data were obtained on an SPS/$CDCl_3$ gel after aging for 1 week at room temperature. Least-squares fitting of eq 8 to the intensity data was performed as shown in Figure 5. The fit is not satisfactory for a large $q$ range, giving the following parameters: $R_g = 65.93$ nm, $\xi' = 34.16$, and $D'_m = 1.99$ ($\nu = 0.50$). The value of $R_g$ seems too large compared with the critical overlap $R_g^*$ (=27.3 nm) value at 0 °C, which is evaluated from the $M_w$ and the critical overlap concentration $C^*$ measured by the

**Table 2. Structural Parameters for SPS Gels Dispersed in Various Solvents Evaluated by Least-Squares Fits of Eq 8 to SANS Data Measured with PSD Located at 10.0 and 1.5 m**

| $M_w$ | solvent | $C$ (g/dL) | $R_g$ (nm) | $D'_m$ | $\xi'$ (nm) | $\nu$ |
|---|---|---|---|---|---|---|
| 360 K | o-DCB | 4.00 | 9.475 | 2.333 | 28.51 | 0.4285 |
| 360 K | $CDCl_3$ | 6.43 | 65.93 | 1.986 | 34.16 | 0.5035 |
| 248 K | $CCl_4$ | 3.96 | 9.233 | 1.995 | 28.51 | 0.5013 |

**Table 3. Structural Parameters for SPS-$d_8$/$CCl_4$ Gels at Various Concentrations Evaluated by Least-Squares Fits of Eq 2' to SANS Data Measured with PSD Located at 10.0 and 1.5 m**

| $M_w$ | solvent | $C$ (g/dL) | $r_0$ (nm) | $D_m$ | $\xi$ (nm) | $D_s$ |
|---|---|---|---|---|---|---|
| | | 0.206 | 4.232 | 1.987 | 47.08 | 2.540 |
| 248 K | $CCl_4$ | 2.02 | 3.849 | 1.855 | 41.09 | 2.787 |
| | | 3.96 | 4.382 | 1.745 | 33.37 | 2.811 |

**Table 4. Structural Parameters for SPS/o-DCB-$d_4$ Gels Different in Molecular Weights ($M_w$) and Concentration Evaluated by Least-Squares Fits of Eq 2' to SANS Data Measured with PSD Located at 4 m**

| $M_w$ | solvent | $C$ (g/dL) | $r_0$ (nm) | $D_m$ | $\xi$ (nm) | $D_s$ |
|---|---|---|---|---|---|---|
| 1135K | o-DCB | 10.0 | 3.968 | 2.274 | 15.34 | 2.226 |
| 400K | o-DCB | 10.0 | 4.910 | 2.202 | 18.15 | 2.365 |
| 150K | o-DCB | 10.0 | 3.960 | 2.270 | 16.03 | 2.569 |
| 1135K | o-DCB | 1.00 | 4.157 | 2.300 | 17.93 | 2.320 |
| 400K | o-DCB | 1.00 | 3.911 | 2.521 | 14.68 | 2.507 |
| 150K | o-DCB | 1.00 | 4.724 | 2.307 | 20.42 | 2.784 |
| 1135K | o-DCB | 0.50 | 4.935 | 2.393 | 18.23 | 2.679 |
| 400K | o-DCB | 0.50 | 4.406 | 2.465 | 15.87 | 2.690 |
| 150K | o-DCB | 0.50 | 4.725 | 2.551 | 15.77 | 2.849 |
| 1135K | o-DCB | 0.10 | 4.969 | 2.552 | 15.62 | 2.928 |
| 400K | o-DCB | 0.10 | 4.641 | 2.598 | 14.36 | |
| 150K | o-DCB | 0.10 | 5.271 | 2.785 | 12.54 | |

tilting method.[13] The $I(q)$ profile of the present SPS/$CDCl_3$ gel seems, as a whole, to situate in between those of a well-developed cluster (a continuous fractal object) and an ensemble of starlike segmental coagulates which entangle each other.

The $I(q)$ data of the SPS/o-DCB-$d_4$ and SPS-$d_8$/$CCl_4$ gels were also analyzed with eq 8. The obtained structural parameters are given in Table 2 for comparison. Since the values of $R_g$ and $\xi'$ are unreasonable ($R_g < \xi'$) and the Flory exponent $\nu$ seems too small, eq 8 is unsuitable for describing the SANS data of well-organized gel networks.

Figure 6 shows the theoretical curves (eq 2' with eqs 3 and 7) fitted to $I(q)$ data of SPS-$d_8$/$CCl_4$ gels at different concentrations. The structural parameters obtained are given in Table 3. With increasing concentration, $\xi$ and $D_m$ decrease, $D_s$ increases, and $r_0$ remains almost constant. Figure 7 shows the results of least-squares fitting to $I(q)$ data (measured at $L$ = 4.0 m) of SPS/o-DCB-$d_4$ gels ($C$ = 1.0 g/dL) of different molecular weights. The structrual parameters obtained are summarized in Table 4 along with their concentration dependence. Because of a comparatively narrow available $q$ range, the values of the parameters deviate more or less from those obtained for the data covering a wider $q$ range (Table 1). Thus for SANS experiments, data covering a wide $q$ range are essentially important for accurate evaluation of structural parameters. Nevertheless, we are able to find some trends of $M_w$ and $C$ dependencies of the parameters; for $r_0$, $\xi$, and $D_m$ there are no systematic dependencies on both $M_w$ and $C$, while $D_s$ tends to decrease (approaching 2.0 for a flat surface) with increasing $M_w$ and $C$.

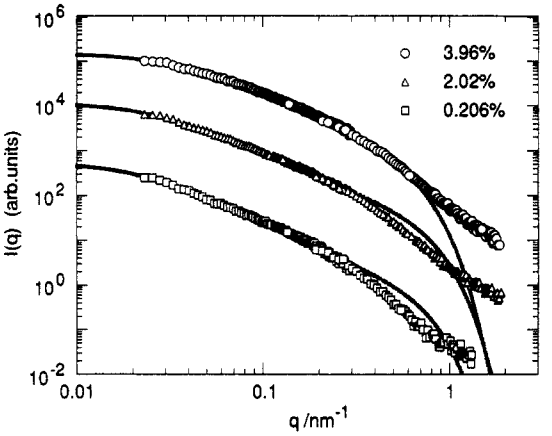


**Figure 6.** Least-squares fitting of eq 2' (with eqs 3 and 7) to the measured $I(q)$ vs $q$ curves shown in Figure 2.

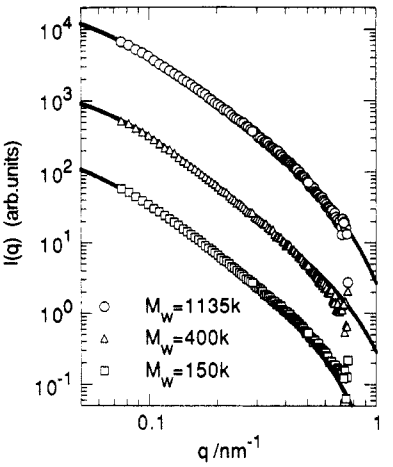


**Figure 7.** Least-squares fitting of eq 2' (with eqs 3 and 7) to the measured $I(q)$ vs $q$ curves (with PSD positioned at $L$ = 4.0 m apart from the sample) for SPS/o-DCB-$d_4$ gels of various molecular weights ($C$ = 1.0 g/dL at 23 °C).

## Comparison with Other Treatments of SANS Data

Analyses of SANS intensity profiles of various polymeric aggregates dispersed in solvents have been made by many authors. In a small $q$ range, $I(q)$ of dilute polymer solutions can be analyzed according to the Guinier equation

$$I(q) = I(0) \exp(-q^2 R_g^2/3) \quad (9)$$

to evaluate the radius of gyration $R_g$. In this way Pachence et al.[19] studied the systems of proteins (enzymes) and their complexes with a detergent micelle dispersed in aqueous solutions containing inorganic salts. For these cases the log $I(q)$ vs $q^2$ plot (the Guinier plot) gave a straight line in a small $q$ range (the Guinier regime). For the present samples, on the contrary, there is no distinct linear region in the Guinier plot as illustrated in Figure 8 for an SPS-$d_8$/$CCl_4$ gel.

Another method commonly used for studying the chain trajectory of polymer molecules in gels is the Kratky plot, i.e., an $I(q)q^2$ versus $q$ plot. Klein et al.[20,21] analyzed the scattering profiles of physical gels of isotactic polystyrene (IPS) dispersed in *cis*- and *trans*-decalin at various polymer concentrations (in a high concentration range of 10–40 g/dL compared with our SPS gels). In order to get information about the chain trajectory in gels, the coherent scattering intensities from labeled (deuterated) IPS molecules embedded in normal IPS gels were investigated. With such a diluted system, we are able to obtain the form factor of the single molecule. In a large $q$ range ($qR_g \gg$

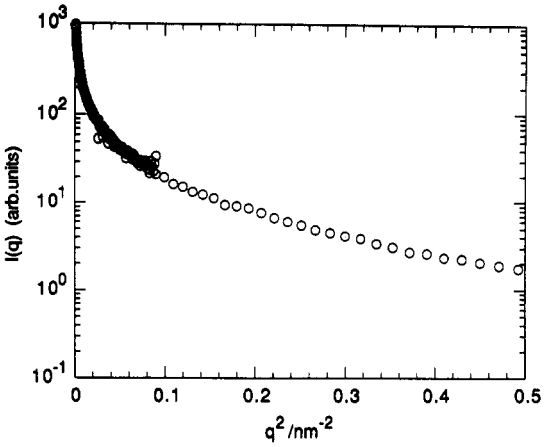


**Figure 8.** Guinier plot of a scattering intensity function for an SPS-$d_8$ ($M_w$ = 25 × 10⁴)/$CCl_4$ gel ($C$ = 3.96 g/dL at 25 °C).

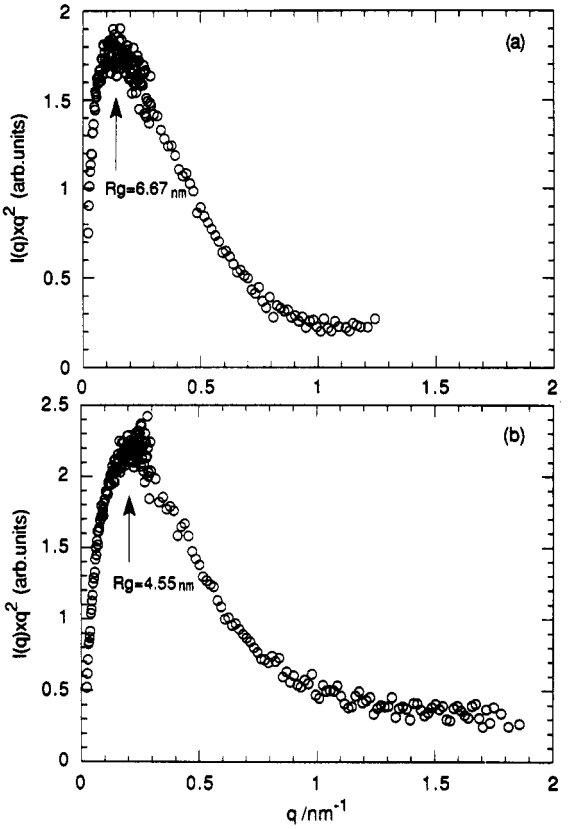


**Figure 9.** Kratky plots of scattering intensity functions for (a) SPS ($M_w$ = 36 × 10⁴)/$o$-DCB-$d_4$ gel ($C$ = 4.00 g/dL) and (b) SPS-$d_8$ ($M_w$ = 25 × 10⁴)/$CCl_4$ gel ($C$ = 3.96 g/dL at 25 °C).

1), the $I(q)$ reduces to

$$I(q) \propto q^{-n} \tag{10}$$

where $1/n = \nu$ is the Flory exponent that depends on the chain trajectory. For a Gaussian chain $\nu = 1/2$ (or $n = 2$), the Kratky plot levels off, causing a plateau region for large $q$. As the chain stiffness increases, the exponent $n$ decreases, approaching unity for the rodlike chain. The Kratky plot of IPS/decalin gels were satisfactorily fitted with wormlike chain trajectories.

For undiluted systems as the present case, the Kratky plot for a gel has a maximum at $qR_g = 1$. From the maximum position the radius of gyration $R_g$ can be evaluated. On the other hand, there appears to be no maximum in the Kratky plot of a sol.

Kratky plots for SPS/$o$-DCB-$d_4$ and SPS-$d_8$/$CCl_4$ gels show a maximum as shown in parts a and b of Figure 9,

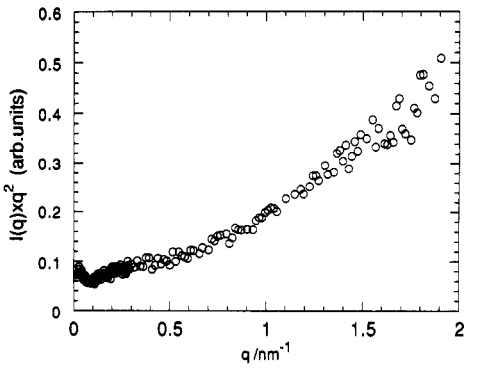


**Figure 10.** Kratky plot of the scattering intensity function for SPS ($M_w$ = 36 × 10⁴)/$CDCl_3$ gel ($C$ = 6.43 g/dL at 25 °C).

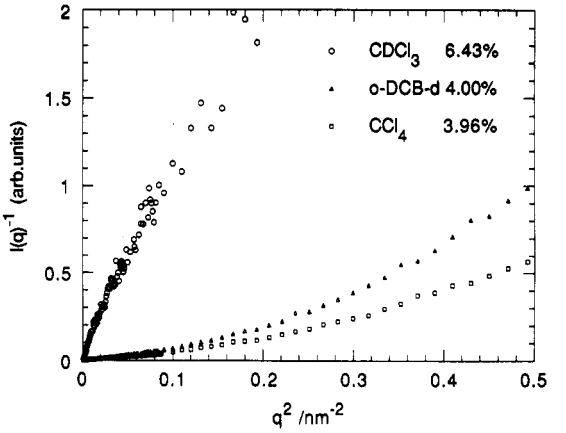


**Figure 11.** Ornstein–Zernike plot of the scattering intensity function for SPS (or SPS-$d_8$) gels dispersed in various solvents.

respectively. The $R_g$ values obtained from the maximum position ($R_g$ = 6.67 nm for an SPS/$o$-DCB-$d_4$ gel and $R_g$ = 4.55 nm for an SPS-$d_8$/$CCl_4$ gel at $C$ = 3.96 g/dL) are smaller than the $R_g$ obtained with eq 8 and larger than the $r_0$ obtained with eq 2′. For an SPS-$d_8$/$CCl_4$ gel, the $R_g$ value estimated from Kratky plots increases with decreasing polymer concentration. In contrast to the above two cases shown in Figure 9, the SPS/$CDCl_3$ gel results in a sol-type Kratky plot (Figure 10), lacking a distinct maximum. This indicates that the cluster formed in this system stays at an early stage of the gelation process, although the substance is apparently immobilized against a shear induced by tilting. On reference to the structural parameters obtained in the preceding section through least-squares fits with eqs 2′ (with eqs 3 and 7) and 8, we may speculate the following structural model. In the matrix of polymer solution, small starlike segmental coagulates are formed and they are separated from one another by rather long distances. Some of them are connected to each other with polymer chains, forming a loosely packed gel network. After being kept at 15 °C for a long time, the same sample causes a gel-type Kratky plot, suggesting that organization of the gel network in this system proceeds with lowering temperature, in parallel to the TTGG conformational ordering of SPS molecules as revealed by infrared spectroscopy.

A commonly used equation for describing SANS intensities from fractal objects is the generalized Zimm equation expressed as

$$I(0)/I(q) = [1 + (D_m + 1)\xi^2 q^2/3]^{D_m/2} \tag{11}$$

For the case of Gaussian chains with $D_m$ = 2, eq 11 is reduced to the Ornstein–Zernike equation

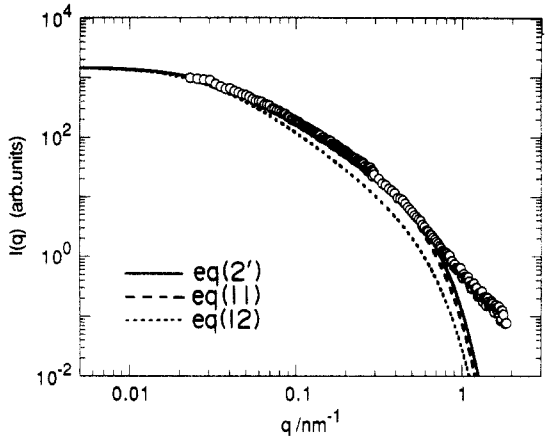


**Figure 12.** Comparison of least-squares fittings of various equations to the measured $I(q)$ vs $q$ curve for an SPS-$d_8$ ($M_w$ = 25 × 10$^4$)/$CCl_4$ gel ($C$ = 4.00 g/dL at 25 °C): (—) eq 2′ (with eqs 3 and 7), (- - -) eq 11, (· · ·) eq 12.

$$I(0)/I(q) = (1 + \xi^2 q^2) \tag{12}$$

The plot of $I(0)/I(q)$ versus $q^2$ gives a straight line and the correlation length $\xi$ can be obtained from the slope.

Kanaya et al. analyzed SANS profiles of poly(vinyl alcohol) (PVA) gels dispersed in mixed solvents of deuterated dimethyl sulfoxide (DMSO-$d_6$) and $D_2O$ according to eq 12.[22] For the $q$ range of 0.3–0.8 nm$^{-1}$, a good linear relationship was obtained and the $\xi$ value was evaluated as a function of temperature.

Shibayama et al.[23] analyzed SANS profiles of PVA–borate aqueous gels according to eq 11 and obtained the $\xi$ value as a function of temperature covering both the gel and sol states.

For the present SPS gels the $I(q)^{-1}$ versus $q^2$ plots are curved in the whole $q$ range investigated and the linear part is limited to a very low $q$ range as shown in Figure 11. Another difficulty in evaluating the $\xi$ value from the plots comes from the ambiguity in the value of $I(0)$ obtained from the intercept at $q$ = 0. Therefore, the results of the least-squares fitting with eq 12 are strongly dependent on the $q$ range used. For the case of the SPS/$CDCl_3$ gel indicated in Figure 11, $\xi$ = 11.02 nm was obtained using the data in $q^2 < 0.3$ nm$^{-2}$, while $\xi$ = 16.71 nm using the data in $q^2 < 0.1$ nm$^{-2}$. For SPS/$o$-DCB-$d_4$ and SPS-$d_8$/$CCl_4$ gels, no reliable $\xi$ values were obtained.

For the cases of the SPS-$d_8$ ($M_w$ = 25 × 10$^4$)/$CCl_4$ gel ($C$ = 4.00 g/dL at 25 °C), the calculated $I(q)$ versus $q$ curves derived by eq 2′ (with eqs 3 and 7) as well as eqs 11 and 12 both multiplied by the form factor (eq 3) (with the same set of structural parameters: $I(0)$ = 1464, $r_0$ = 4.382 nm, $D_m$ = 1.745, and $\xi$ = 33.37 nm) are compared with the experimental result (Figure 12).

## References and Notes

(1) Natta, G.; Pino, P.; Corradini, P.; Danusso, F.; Mantia, E. *J. Am. Chem. Soc.* **1955**, *77*, 1700.
(2) Immirzi, A.; de Candia, F.; Ianneli, P.; Zambelli, A.; Vittoria, V. *Makromol. Chem., Rapid Commun.* **1988**, *9*, 761.
(3) Vittoria, V.; de Candia, F.; Ianneli, P.; Immirzi, A. *Makromol. Chem., Rapid Commun.* **1988**, *9*, 765.
(4) Kobayashi, M.; Nakaoki, T.; Ishihara, N. *Macromolecules* **1989**, *22*, 4377.
(5) Chatani, Y.; Fujii, Y.; Shimane, Y.; Ijitsu, T. *Polym. Prepr. Jpn. (Engl. Ed.)* **1988**, *37*, E428.
(6) Guerra, G.; Vitagliano, V. M.; De Rosa, C.; Petraccone, V.; Corradini, P. *Macromolecules* **1990**, *23*, 1539.
(7) Corradini, P.; Napolitano, R.; Pirozzi, B. *Eur. Polym. J.* **1990**, *26*, 157.
(8) Greis, O.; Xu, Y.; Asano, T.; Petermann, J. *Polymer* **1989**, *30*, 590.
(9) Chatani, Y.; Shimane, Y.; Inoue, Y.; Inagaki, T.; Ishioka, T.; Ijitsu, T.; Yukinari, T. *Polymer* **1992**, *33*, 488.
(10) Kobayashi, M.; Nakaoki, T.; Ishihara, N. *Macromolecules* **1990**, *23*, 78.
(11) Nakaoki, T.; Kobayashi, M. *J. Mol. Struct.* **1991**, *242*, 315.
(12) Nakaoki, T.; Kobayashi, M. *Rep. Progr. Polym. Phys. Jpn.* **1990**, *33*, 91.
(13) Nakaoki, T.; Kozasa, T.; Kobayashi, M. *Rep. Progr. Polym. Phys. Jpn.* **1992**, *35*, 129.
(14) Kobayashi, M.; Kozasa, T. *Appl. Spectrosc.* **1993**, *47*, 1417.
(15) Ishihara, N.; Seimiya, T.; Kuramoto, M.; Uoi, M. *Macromolecules* **1986**, *19*, 2464.
(16) Freltoft, T.; Kjems, J. K.; Sinha, S. K. *Phys. Rev. B* **1986**, *33*, 269.
(17) Kobayashi, M.; Yoshioka, T.; Imai, M.; Ito, Y. *J. Chem. Phys.*, to be published.
(18) Dozier, W. D.; Huang, J. S.; Fetters, L. J. *Macromolecules* **1991**, *24*, 2810.
(19) Pachence, J. M.; Edelman, I. S.; Schoenborn, B. P. *Biol. J. Chem.* **1987**, *262*, 702.
(20) Klein, M.; Brulet, A.; Guenet, J.-M. *Macromolecules* **1990**, *23*, 540.
(21) Klein, M.; Guenet, J.-M.; Brulet, A. *Polymer* **1991**, *32*, 1943.
(22) Kanaya, T.; Ohkura, M.; Kaji, K.; Furusaka, M.; Misawa, M.; Yamaoka, H.; Wingnall, G. D. *Physica* **1992**, *B180 & 181*, 549.
(23) Shibayama, M.; Kurokawa, H.; Nomura, S.; Mutherukumar, M.; Stein, R. S.; Roy, S. *Polymer* **1992**, *33*, 2883.